



Supplementary Information for

The antiquity of forelimb ecomorphological diversity in the mammalian stem lineage
(Synapsida)

Jacqueline K Lungmus, Kenneth D Angielczyk

Jacqueline K Lungmus
Email: jlungmus@uchicago.edu

This PDF file includes:

Supplementary text
Figs. S1 to S5
Tables S1 to S5
Caption for SI Appendix Dataset
References for SI citations

Other supplementary materials for this manuscript include the following:

S2 Appendix Dataset

Supplemental Methods

Temporal and Taxonomic sampling

A full list of the sampled genera is provided in SI Appendix Dataset. The “pelycosaur” clade Eothyrididae is represented by one distal humerus referable to the *Baldwinonius trux* (MCZ1650). This single distal humerus contributes to the total disparity values and the within-group treatments for the times bins in which it is present (305 & 300 mya), but does not allow a separate treatment of eothyridid disparity. The distal end of a single specimen of *Ruthenosaurus russellorum* (MNHN.F.MCL-1) was digitized during data collection, but was not included in the final analyses because of the uncertainty surrounding its age (1). However, the specimen is noteworthy in having a unusual distal humerus shape and would likely increase pelycosaur distal humerus disparity if its time bin could be accurately assigned.

Time range data for the specimens were designated at the species level for those specimens that had confident species identifications. Specimens that could only be identified at a higher taxonomic level were given bin placements for the entire time range of the most precise identification possible (e.g., each time bin in which a genus occurs). Specimens that could not be identified to genus were excluded from the analysis. The singular exception is a gorgonopsian humerus from a historic and well studied forelimb (Cambridge University Museum of Zoology No. T.883). This specimen was given a stratigraphic bin assignments that represent the range of possible ages for Gorgonopsia. Bin placement is defined as a time range, with “presence” being designated if the taxon that the specimen represents was present at any point during the 5 million year time span.

Non-mammalian synapsids are the stem lineage of the mammalian crown-group. As such the two subgroups of synapsids examined in this study (pelycosaurs and therapsids) are paraphyletic assemblages. Pelycosaurs comprise the grade of synapsids on the stem of Therapsida. Therapsida is a monophyletic clade that includes stem-lineage non-mammalian therapsids and mammals. Our work focuses on the paraphyletic assemblage of non-mammalianform therapsids from the Permian and Triassic periods, exclusive of mammals and their close relatives (mammaliaforms). We consider this approach justified because pelycosaurs and therapsids are two important, temporally-successive evolutionary radiations of synapsids. Our focus on pelycosaurs and therapsids

is comparable to analyses of non-avian dinosaurs exclusive of birds. Pelycosaur and therapsids overlapped temporally during their evolutionary history, and that overlap occurs in two time bins in the analysis (270 and 265 Mya).

There is no comprehensive phylogeny of non-mammalian synapsids that includes all of the taxa examined in this analysis. To investigate possible phylogenetic effects on the disparity signal we built a composite phylogeny by hand using a variety of literature sources for relationships within and among subclades as follows: pelycosaurs: Berman et al. (2014)(2), Brocklehurst et al. (2015)(3); relationships among major therapsid clades: Sidor and Hopson (1998)(4); Dinocephalia: Rubidge and van den Heever (1997)(5); Anomodontia: Kammerer (2018)(6); Therocephalia: Huttenlocker and Smith (2017)(7); Cynodontia: Ruta et al. (2013)(8), Van den Brandt and Abdala (2018)(9), Pavanatto et al. (2018)(10). Stratigraphic ranges for the included taxa were collected from the PBDB (SI Appendix Dataset), and a time tree was produced in R using the Claddis package (11) using minimum branch length. We then conducted a multivariate phylogenetic least squares regression using mean genus shapes, treating centroid size as a covariate, and the time tree in Geomorph (12). Results showed no significant influence of phylogeny on mean shape (proximal Pagel's $\lambda = 0.3807071$, $p = 0.445$; distal Pagel's $\lambda = 0.2887207$, $p = 0.429$). Tree topology used for the analysis can be viewed in SI Appendix Fig.S1 and SI Appendix Fig.S2. A generalized distancing analysis was conducted to confirm that the disparity pattern was not being driven by a bias in the number of groups from bin to bin. Results using both Spearman's rho and Kendall's tau show that sample size is not correlated with the disparity (p values – distal = 0.8651, 0.9647; proximal = 0.1447, 0.1949).

Phylogenetic evidence implies a long therapsid ghost lineage that is not included in our analyses (13). The pelycosaur clade Sphenacodontidae is widely considered to be the sister group of Therapsida (13,14), and the Pennsylvanian first appearance of Sphenacodontidae implies that therapsids must have diverged by that time. However, there are no known Pennsylvanian therapsid fossils, and the only potential early Permian record of Therapsida is controversial and consists only of cranial material (15,16,17). This implies that therapsids could have had a long and undocumented period of time to accumulate the forelimb disparity the group displays when it first appears in our sample.

However, the absence of Permo-Carboniferous therapsids does not allow us to determine whether therapsids initially were characterized by a pelycosaur-like low level of humeral disparity that gradually increased across this time interval, or if disparity rapidly increased near their definitive first appearance in the fossil record in the middle Permian, or at a different time in their history (e.g., a rapid increase shortly after their divergence from sphenacodontids). Regardless of timing, the high disparity coincident with the emergence of Therapsida in our dataset is clearly related to critical differences in forelimb morphology and inferred function compared to pelycosaurs. As discussed in the Main Text, the appearance of novel morpho-functional types is a hallmark of therapsid evolution from the middle Permian onwards, and is observable across much of the therapsid body plan. Determining whether this property of therapsids is the result of changes in selection pressures, developmental mechanisms, other factors that occurred in the middle Permian, or is the culmination of evolutionary changes that had been accumulating “off-stage” since the Pennsylvanian, will require the discovery of Permo-Carboniferous therapsid fossils. Likewise, attempts to infer rates and models of evolution during the early history of therapsids using currently available fossils and phylogenetic data is suspect because the results would be unconstrained by fossil data for the therapsid lineage (see Mitchell, 2015 (18) for a comparable example in birds).

Geometric morphometric and disparity methods

Analyses were split between the two ends of the humerus because of the dramatic degree of long axis twisting in many pelycosaur and therapsid humeri. This twisting prevents a single two-dimensional view from capturing details of both articulation surfaces. Moreover, the degree of twisting is frequently affected by taphonomic deformation (i.e., it can be reduced or exaggerated depending on the direction in which a specimen experienced compression), potentially biasing three-dimensional data that could theoretically capture the entire humeral shape. The approach of splitting the humerus into two functional ends had the added benefit of maximizing sample size because it allowed the inclusion of humeri in which one end was intact but the other was damaged or missing. Finally, separate consideration of the shapes of the two sections of the humerus

contributed to the unique finding that the proximal end of the humerus represents a disproportionate amount of therapsid humeral disparity.

95 A Procrustes ANOVA was used to assess the covariation between shape coordinates and log centroid size, with residual randomization (summary and significance in IAppendix, Table S4). The results of the analysis revealed that size was a significant predictor of shape for both humeral ends. Because of this, the centroid size of each specimen (or genus in the case of mean shapes) was treated as a known covariate during
100 the regression analysis. Data were visualized with a principal components analysis, and an expanded set of PC axes are presented in SI Appendix Fig. S3 and SI Appendix Fig. S4, along with an associated scree plot of variance captured by each PC (SI Appendix, Fig. S5).

All disparity values reported and plotted in Main Text Fig.2A-C were measured
105 as Procrustes variance directly upon the multivariate geometric morphometric data. Procrustes variance is the sum of the diagonal elements of the covariance matrix of a defined group, divided by the number of occurrences within that group (12,19,20). Research comparing the effects of sampling on various disparity metrics shows that variance-based metrics are relatively immune to biases caused by small sample size
110 (21,22). Regardless, the total-group disparity values were additionally analyzed to understand the amount of error present in the results. The sample of genera present during each time bin were randomly resampled with replacement to the same sample size as the true dataset in that given time bin, this new simulated sample subsequently underwent a morphological disparity analysis in the 'R' geomorph package. This random
115 resampling and conducting of a new disparity analysis was conducted 1,000 times for each time bin, and the variation in those results were used to calculate the standard deviation of each time bin.

The Permo-Triassic mass extinction is hypothesized to have taken place 252.24 Mya (23). The Permo-Triassic Mass Extinction event is designated as a time bin at 252
120 Mya, and represents the fauna immediately post-extinction, capturing both survivors and new taxa in the immediate disaster fauna. Given the severity of the extinction event, the finding that distal humeral disparity does not decrease in this time interval is counterintuitive. Detailed analysis conducted upon the individual specimens present

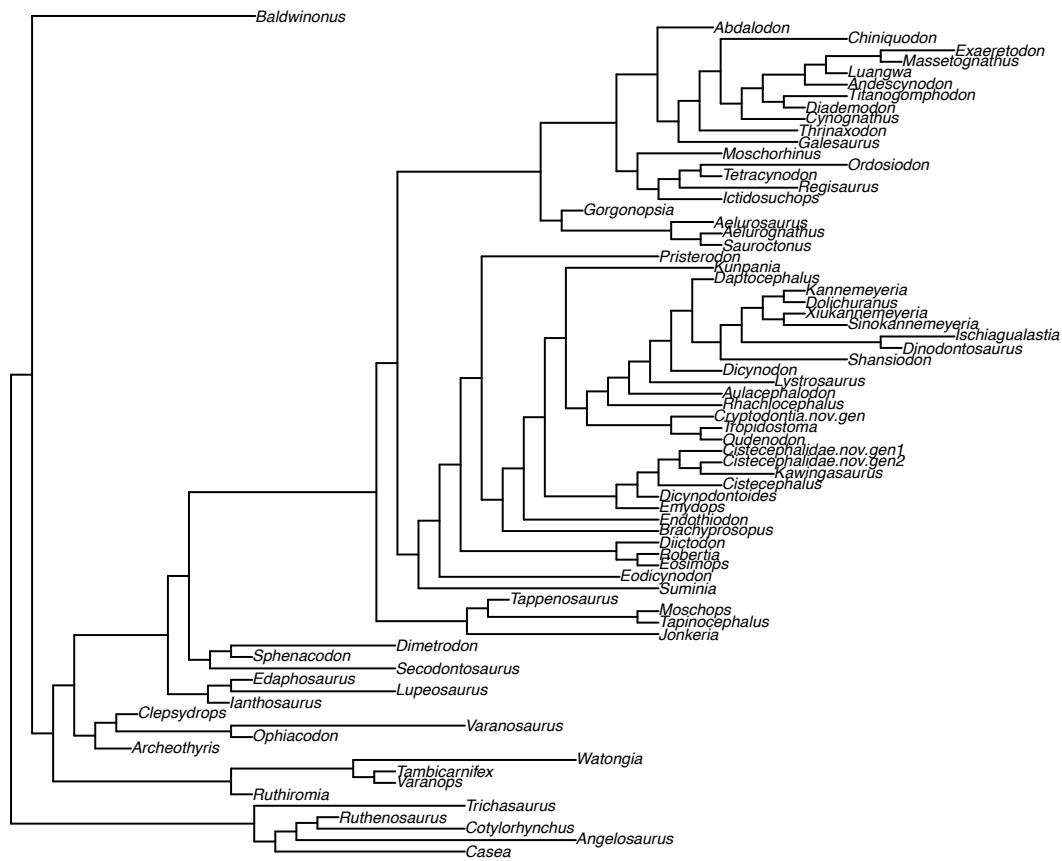
across the interval revealed that the clearing of morphospace resulting from the extinction
 125 occurred primarily in the intermediate areas of morphospace, whereas the survivors are
 derived groups that occupy the periphery of morphospace (such as Therocephalia).
 Combined with the overall decrease in sample size across the extinction, this results in
 the average distance from the total group mean increasing in the distal end of the
 humerus. Results show an expected effect of the mass extinction event for proximal
 130 humeral morphology, with decreases across the extinction interval. Following this,
 disparity values imply a rediversification in limb disparity as both end of the humerus
 increase beyond pre-extinction levels of morphological disparity (Main Text Fig.2A).

Museum abbreviations

135 Abbreviations for museum institutions associated with specimen numbers are as follows:

- AMNH - American Museum of Natural History, New York, USA
- BP – Evolutionary Studies Institute, University of the Witwatersrand, Johannesburg,
South Africa
- 140 CNHM - Cleveland Museum of Natural History, Cleveland, OH, USA
- CMZ - University Museum of Zoology, Cambridge, UK
- FMNH - Field Museum of Natural History, Chicago, IL, USA
- GPIT - Paläontologische Sammlung, Eberhard Karls Universität Tübingen, Tübingen,
Germany
- 145 IVPP - Institute of Paleoanthropology and Paleontology, Beijing, China
- KUVP - University of Kansas Natural History Museum, Lawrence, KA, USA
- MCZ - Museum of Comparative Zoology, Cambridge, MA, USA
- MNG - Museum der Natur, Gotha, Germany
- MNHN - Muséum national d'Histoire naturelle, Paris, France
- 150 NHCC - National Heritage Conservation Commission, Lusaka, Zambia
- NHMUK - Natural History Museum, London, UK
- NMB - Natural History Museum of Basel, Basel, Germany
- NMT - National Museum of Tanzania, Dar es Salaam, Tanzania
- NMQR - National Museum, Bloemfontein, South Africa
- 155 OUMNH - University of Oklahoma Sam Noble Museum, Norman, OK, USA
- PIN - Paleontological Institute of the Russian Academy of Sciences, Moscow, Russia
- PVL - Instituto Miguel Lillo, Tucumán, Argentina
- SAM – Iziko South African Museum, Cape Town, South Africa
- TMM - Texas Memorial Museum, Austin, TX, USA
- 160 UCMP - University of California Museum of Paleontology, Berkeley, CA, USA

USNM - National Museum of Natural History (Smithsonian Institution), Washington
D.C., USA



165

Figure S1 - Phylogeny used to test for phylogenetic signal in proximal humeral morphology. Details of tree construction are in SI Appendix section *Temporal and Taxonomic Sampling*.

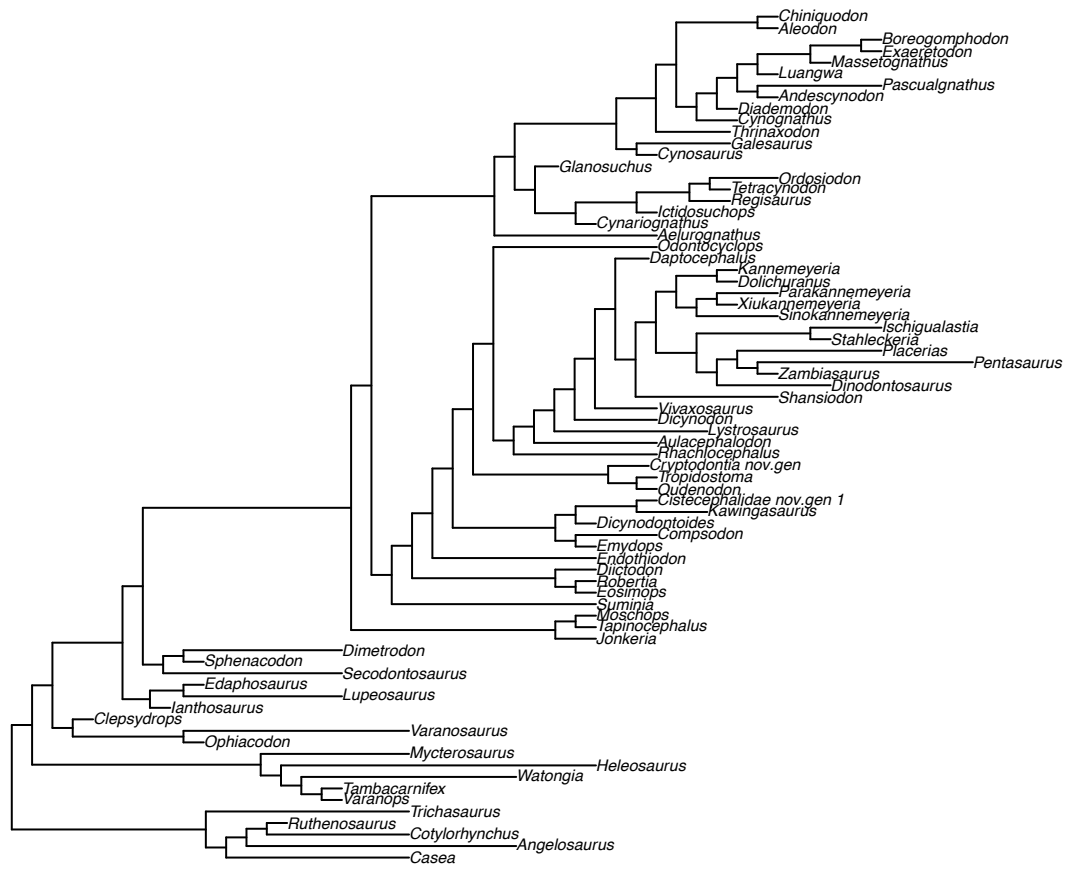


Figure S2 - Phylogeny used to test for phylogenetic signal in proximal humeral morphology. Details of tree construction are in SI Appendix section *Temporal and Taxonomic Sampling*.

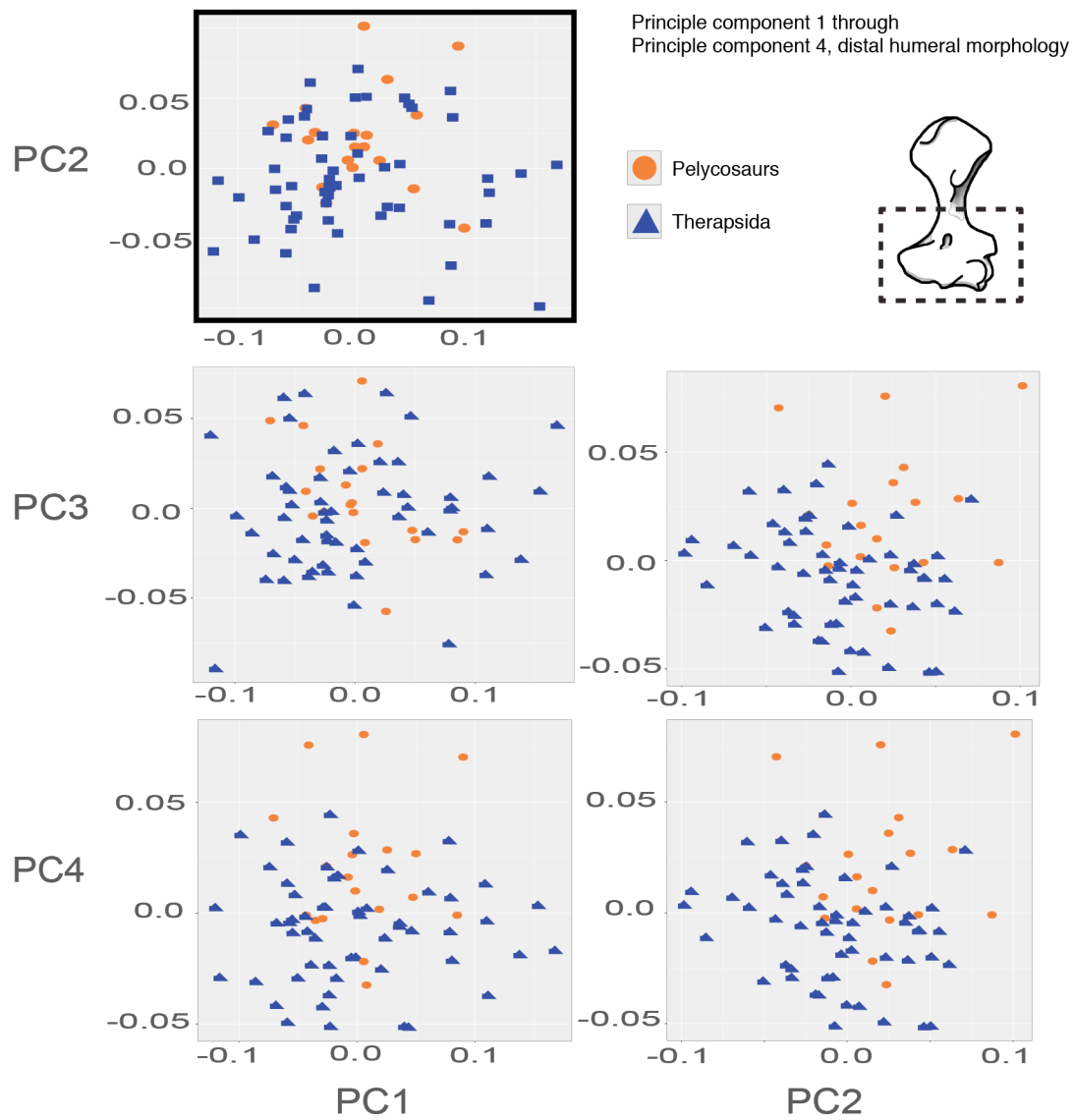
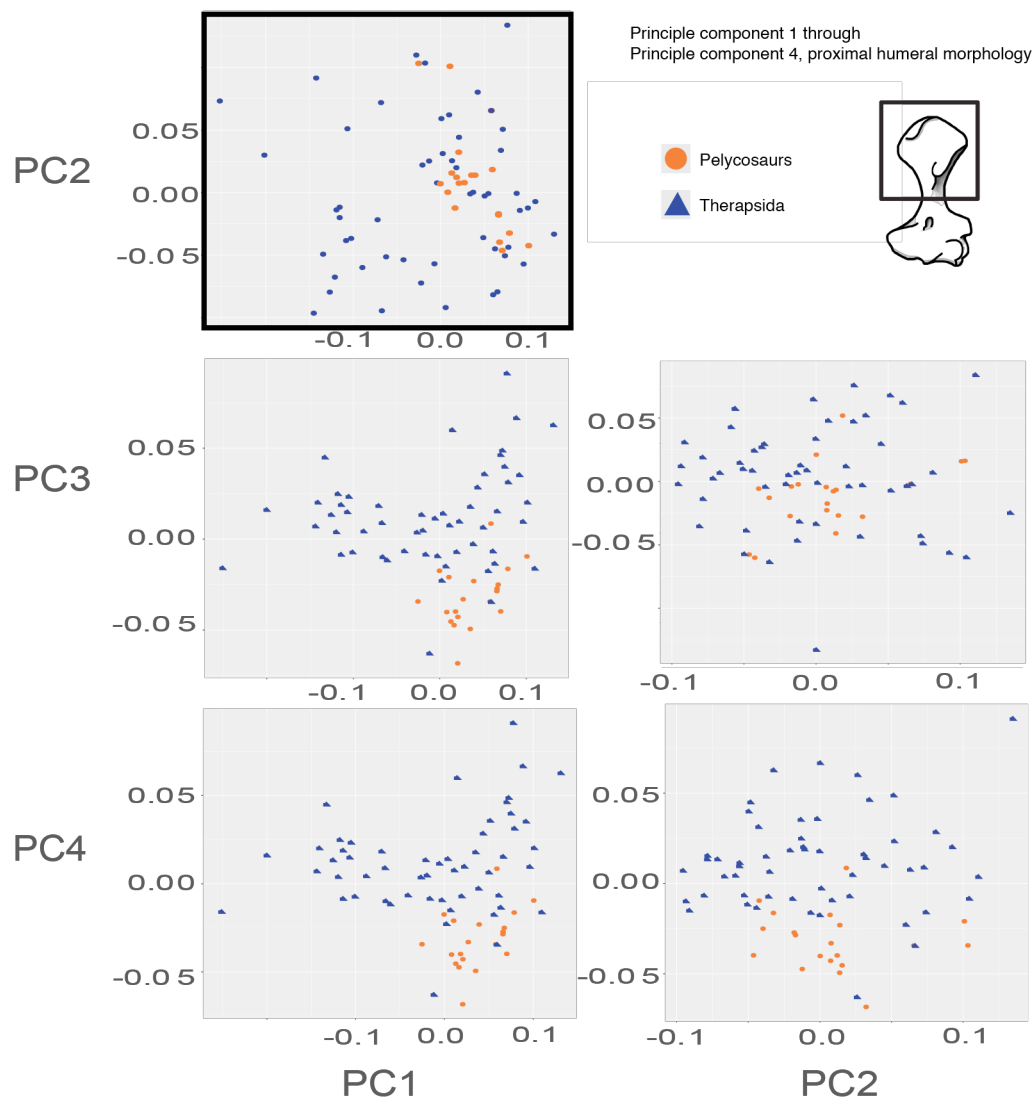


Fig. S3. Distal end morphospaces of PC1 through PC4. Colored by clad: orange circles are “pelycosaurs” and blue triangles are therapsids. Black box highlights the plot reported in the Main Text Figure 1B.



185

Fig. S4. Proximal end morphospaces of PC1 through PC4. Colored by clade: orange circles are “pelycosaurs” and blue triangles are therapsids. Black box highlights the plot reported in the Main Text Figure 1B.

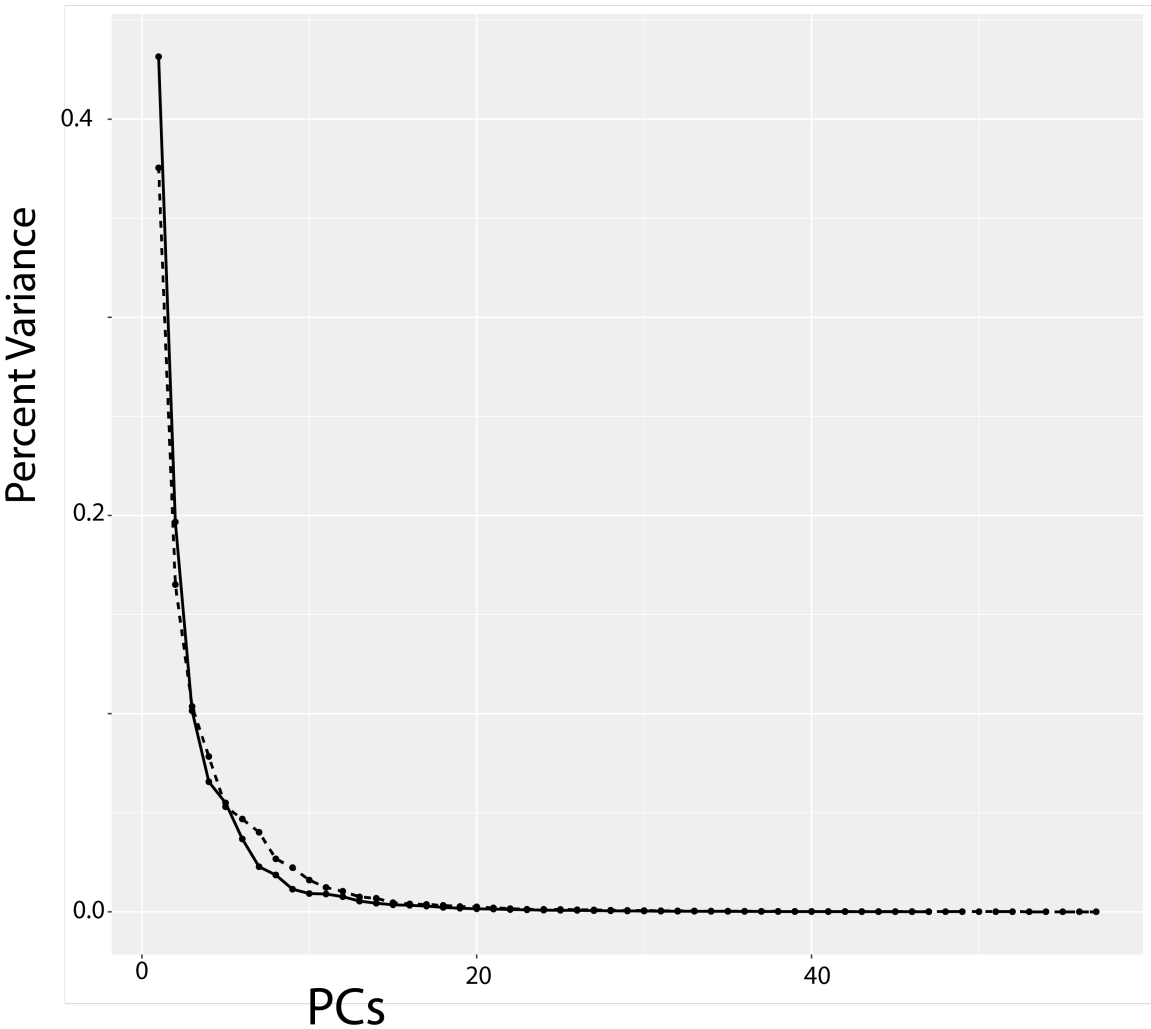


Fig. S5. Skree plot showing percent variance of principle components axes for distal (dashed line) and proximal (solid line) ends.

Table S1. Taxonomic identifications associated with Figure1A (Main Text)

Number in F1	Specimen number	Identification
1	FMNH UR 581	<i>Cotylorhynchus hancocki</i>
2	MCZ 1486	<i>Ophiacodon retroversus</i>
3	MCZ 3417	<i>Edaphosaurus</i> sp.
4	USNM 6723	<i>Dimetrodon limbatus</i>
5	FMNH UR 2483	<i>Jonkeria</i> sp.
6	BP/1/4086	<i>Cistecephalus microrhinus</i>
7	PVL 3807	<i>Ishigualastia jenseni</i>
8	SAM-PK-K1676	Gorgonopsia
9	MCZ 3691	<i>Massetognathus pascuali</i>

Table S2. Full Procrustes variance values for each time bin associated with Figure2A (Main Text)

Time Bin	Pelycosaur		Therapsid	
	Proximal	Distal	Proximal	Distal
305 mya	0.005113621	0.004017046		
300 mya	0.004070158	0.001291970		
295	0.004131235	0.001291970		
290	0.003902196	0.003456816		
285	0.004451662	0.004536993		
280	0.005199914	0.005631861		
275	0.006574254	0.005572765	0.004988890	
270	0.006300588	0.008591300	0.011434922	
265			0.009116469	0.005364114
260			0.013204671	0.007642401
255			0.01458609	0.008900727
252			0.010047123	0.009942058
245			0.013507737	0.010449260
240			0.01266810	0.008314050
235			0.009441241	0.005277366

Table S3. Placement of Landmarks

Humeral end	Landmark #	Placement
Proximal morphology	1	Proximal lateral end of diaphysis
	2	Medial edge of humeral head
	3	Ventral-most extent of deltopectoral rest
	4	Distal-most extent of deltopectoral crest
Distal morphology	1	Anterior distal end of diaphysis
	2	Middle of entepicondyle
	3	Anterior edge of ulnar condyle
	4	Posterior edge of ulnar condyle
	5	Distal edge of ectepicondyle
	6	Middle of ectepicondyle
	7	Proximal edge of ectepicondyle
	8	Posterior distal end of diaphysis

Table S4. Summary and Significance of Procrustes ANOVA

		Df	SS	F	Z	P value
Proximal	log(size)	1	0.13428	10.187	3.6551	0.009901
	Total	71	0.93588			
Distal	log(size)	1	0.03089	3.161	2.3782	0.0198
	Total	71	0.69376			

215 **Table S5. Citations for illustrations used in geometric morphometric analyses**

Citation	Figure number	Specimen number	Specimen ID
(24)	2	KUVP 69035	<i>Ianthasaurus hardestii</i>
(25)	1	KUVP 133735	<i>Ianthodon schultzei</i>
(26)	6	SAM-PK-K8305	<i>Heleosaurus scholtzi</i>
(27)	4	OMNH 52368	<i>Mycterosaurus</i> sp.
(28)	5.5	MNG 10596	<i>Tambicarnifex unguifalcatus</i>
(29)	11	TMM 43628-1	<i>Varanops brevirostris</i>
(30)	2	UCMP 143478	<i>Watongia meieri</i>
(31)	26	NMB C.2693	? <i>Cynognathus</i> sp.
(31)	28	SAM-PK-K1395	<i>Thrinaxodon liorhinus</i>
(32)	10	N/A	<i>Moschops</i> sp.
(33)	7	NHMUK 23345	<i>Eosimops newtoni</i>
(34)	4	GPIT K55	<i>Kawingasaurus fossilis</i>
(35)	4	SAM-PK-11885	<i>Robertia broomiana</i>
(36)	41	CMZ T883	Indet. Gorgonopsian
(37)	28	AMNH 2240	<i>Lycaenops ornatus</i>
(38)	4	SAM-PK-K7809	<i>Glanosuchus macrops</i>
(39)	6	BP/1/3973	<i>Regisaurus</i> sp
(40)	2	NMQR 3605	<i>Olivierosuchus parringtoni</i>

Additional data table SI Appendix Dataset (separate file)

Microsoft excel document with 6 associated sheet pages:

Sheet 1 - Landmark coordinates of total sample, in TPS format. Consistent with TPS format, each specimen is represented by two rows of coordinates, x on the left and y on the right. Each new specimen begins with a line stating the number of landmarks, represented by "LM=". This is followed by number of "Curves", which reflects the number of line segments across which semilandmarks are placed. Immediately following are the x-y coordinates of each semilandmark ("Points="), separated by which curve they pertain to. Lastly, "Image=" is the specimen identifier used for the computational analyses and the scale recorded for each specimen. On the left side of the sheet is data for the proximal humerus, and on the right is the distal humerus.

Sheet 2 - List of taxonomic groups sampled and time-binning for distal morphology, including genera used as averages and singletons included.

Sheet 3 - List of taxonomic groups sampled and time-binning for proximal morphology, including genera used as averages and singletons.

Sheet 4 - Stratigraphic ranges used for analyses.

Sheet 5 - List of specimens used for proximal mean shape analysis.

Sheet 6 - List of specimens used for distal shape analysis.

References

1. Reisz RR, Maddin HC, Fröbisch J, Falconnet J (2011) A new large caseid (Synapsida, Caseasauria) from the Permian of Rodez (France), including a reappraisal of "Casea" rutena Sigogneau-Russell & Russell, 1974. *Geodiversitas* 33(2):227–246.
2. Berman, David S., et al. "First European record of a varanodontine (Synapsida: Varanopidae): Member of a unique Early Permian upland paleoecosystem, Tambach Basin, central Germany." *Early evolutionary history of the Synapsida*. Springer, Dordrecht, 2014. 69-86.
3. Brocklehurst N, Reisz RR, Fernandez V, Fröbisch J (2016) A re-description of "Mycterosaurus" smithae, an early Permian eothyridid, and its impact on the phylogeny of pelycosaurian-grade synapsids. *PLoS One* 11(6):e0156810.
4. Sidor, Christian A., and James A. Hopson. "Ghost lineages and "mammalness": assessing the temporal pattern of character acquisition in the Synapsida." *Paleobiology* 24.2 (1998): 254-273.
5. Rubidge, Bruce S., and Juri A. Van Den Heever. "Morphology and systematic position of the dinocephalian Styraeocephalus platyrhynchus." *Lethaia* 30.2 (1997): 157-168.
6. Kammerer, Christian F., and Kenneth D. Angielczyk. "A proposed higher taxonomy of anomodont therapsids." *Zootaxa* 1.24 (2018): 2009.
7. Huttenlocker, Adam K., and Roger MH Smith. "New whaitsioids (Therapsida: Therocephalia) from the Teekloof Formation of South Africa and therocephalian diversity during the end-Guadalupian extinction." *PeerJ* 5 (2017): e3868.
8. Ruta M, Botha-Brink J, Mitchell SA, Benton MJ (2013) The radiation of cynodonts and the ground plan of mammalian morphological diversity. *Proc Biol*

Sci 280(1769):20131865.

- 265 9. van den Brandt, Marc, and Fernando Abdala. "Cranial morphology and
phylogenetic analysis of *Cynosaurus suppostus* (Therapsida, Cynodontia) from the
upper Permian of the Karoo Basin, South Africa." (2018).
10. Pavanatto, Ane Elise Branco, et al. "A new Upper Triassic cynodont-bearing
fossiliferous site from southern Brazil, with taphonomic remarks and description of
270 a new traversodontid taxon." *Journal of South American Earth Sciences* 88 (2018):
179-196.
- 11.. Lloyd GT (2015) Claddis: an R package for performing disparity and rate analysis
on cladistic-type data sets. *Online GitHub See [https://github](https://github.com/graemetlloyd/Claddis)*
com/graemetlloyd/Claddis.
- 275 12. Adams DC, Otárola-Castillo E (2013) geomorph: an R package for the collection
and analysis of geometric morphometric shape data. *Methods Ecol Evol* 4(4):393–
399.
13. Angielczyk, K.D. and Kammerer, C. F. 2018. Non-mammalian synapsids: the deep
roots of the mammalian family tree. Pp. 117-198 in Zachos, F. E. and Asher R. J.
280 (eds.); *Handbook of Zoology: Mammalia: Mammalian Evolution, Diversity and*
Systematics. De Gruyter, Berlin.
14. Kemp TS (2012) The Origin and Radiation of Therapsids. *Forerunners of*
Mammals, ed Chinsamy-Turan A (Indiana University Press), pp 3–32.
15. Laurin M, Reisz RR (1990) *Tetraceratops* is the oldest known therapsid. *Nature*
345(6272):249–250.
16. Liu J, Rubidge B, Li J (2009) New basal synapsid supports Laurasian origin for
285 therapsids. *Acta Palaeontol Pol* 54(3):393–400.
17. Liu J, Rubidge B, Li J (2010) A new specimen of *Biseridens qilianicus* indicates
its phylogenetic position as the most basal anomodont. *Proc R Soc London B Biol*
Sci 277(1679):285–292.
18. Mitchell JS (2015) Extant-only comparative methods fail to recover the disparity
290 preserved in the bird fossil record. *Evolution (N Y)* 69(9):2414–2424.
19. Rohlf FJ (2010) tpsDig, version 2.12. Stony Brook, NY: Department of Ecology
and Evolution, State University of New York at Stony Brook.
20. Zelditch ML, Swiderski DL, Sheets HD (2012) *Geometric Morphometrics for*
Biologists: A Primer (Academic Press).
- 295 21. Wills MA, Briggs DEG, Fortey RA (1994) Disparity as an evolutionary index: a
comparison of Cambrian and Recent arthropods. *Paleobiology* 20(2):93–130.
22. Brusatte SL, Butler RJ, Prieto-Márquez A, Norell MA (2012) Dinosaur
morphological diversity and the end-Cretaceous extinction. *Nat Commun* 3:804.
23. Burgess SD, Muirhead JD, Bowring SA (2017) Initial pulse of Siberian Traps sills
300 as the trigger of the end-Permian mass extinction. *Nat Commun* 8.
24. Reisz RR, Berman DS (1986) *Ianthasaurus hardestii* n. sp., a primitive edaphosaur
(Reptilia, Pelycosauria) from the Upper Pennsylvanian Rock Lake Shale near
Garnett, Kansas. *Can J Earth Sci* 23(1):77–91.
- 305 25. Spindler F, Scott D, Reisz RR (2015) New information on the cranial and
postcranial anatomy of the early synapsid *Ianthodon schultzei* (Sphenacomorpha:
Sphenacodontia), and its evolutionary significance. *Mitteilungen aus dem Museum*
für Naturkd Berlin Foss Rec 18(1):17.

26. Botha-Brink J, Modesto SP (2009) Anatomy and relationships of the Middle Permian varanopid *Heleosaurus scholtzi* based on a social aggregation from the Karoo Basin of South Africa. *J Vertebr Paleontol* 29(2):389–400.
27. Reisz RR, Wilson H, Scott D (1997) Varanopseid synapsid skeletal elements from Richards Spur, a Lower Permian fissure fill near Fort Sill, Oklahoma. *Oklahoma Geol Notes* 57(5):160–170.
28. Berman DS, Henrici AC, Sumida SS, Martens T, Pelletier V (2014) First European Record of a Varanodontine (Synapsida: Varanopidae): Member of a Unique Early Permian Upland Paleoecosystem, Tambach Basin, Central Germany (Springer, Dordrecht), pp 69–86.
29. Campione NE, Reisz RR (2010) *Varanops brevirostris* (Eupelycosauria: Varanopidae) from the Lower Permian of Texas, with discussion of varanopid morphology and interrelationships. *J Vertebr Paleontol* 30(3):724–746.
30. Reisz RR, Laurin M (2004) A reevaluation of the enigmatic Permian synapsid *Watongia* and of its stratigraphic significance. *Can J Earth Sci* 41(4):377–386.
31. Jenkins FA (1971) Part One: Postcranial Axial Skeleton. *The Postcranial Skeleton of African Cynodonts* (Peabody Museum of Natural History, New Haven), pp 1–91. 36th Ed.
32. Gregory WK, Broom R (1926) *The Skeleton of Moschops Capensis Broom: A Dinocephalian Reptile from the Permian of South Africa* (order of the Trustees, the American Museum of Natural History).
33. Angielczyk KD, Rubidge BS (2013) Skeletal morphology, phylogenetic relationships and stratigraphic range of *Eosimops newtoni* Broom, 1921, a pylaecephalid dicynodont (Therapsida, Anomodontia) from the Middle Permian of South Africa. *J Syst Palaeontol* 11(2):191–231.
34. Cox CB (1972) A new digging dicynodont from the Upper Permian of Tanzania. *Stud Vertebr Evol Oliver Boyd, Edinburgh*:173–189.
35. King GM (1981) *The postcranial skeleton of Robertia broomiana, an early dicynodont (Reptilia, Therapsida) from the South African Karoo* (South African Museum).
36. Kemp TS (1982) *Mammal-like reptiles and the origin of mammals* (Academic Pr).
37. Colbert EH, Broom R (1948) The mammal-like reptile *Lycaenops*. Bulletin of the AMNH; v. 89, article 6.
38. Fourie H, Rubidge BS (2009) The postcranial skeleton of the basal therocephalian *Glanosuchus macrops* (Scylacosauridae) and comparison of morphological and phylogenetic trends amongst the Theriodontia.
39. Fourie H, Rubidge BS (2007) The postcranial skeletal anatomy of the therocephalian *Regisaurus* (Therapsida: Regisauridae) and its utilization for biostratigraphic correlation.
40. Botha-Brink J, Modesto SP (2011) A new skeleton of the therocephalian synapsid *Olivierosuchus parringtoni* from the Lower Triassic South African Karoo Basin. *Palaeontology* 54(3):591–606.